The Astrophysical Journal, 629:825–831, 2005 August 20

DIRECT DETERMINATION OF THE SPIRAL PATTERN ROTATION SPEED OF THE GALAXY

Wilton S. Dias[1] and J. R. D. Lépine[2]
Received 2005 February 11; accepted 2005 April 28

ABSTRACT

The rotation velocity of the spiral pattern of the Galaxy is determined by direct observation of the birthplaces of open clusters of stars in the Galactic disk as a function of their age. Our measurement does not depend on any specific model of the spiral structure, such as the existence of a given number of spiral arms, or the presence of a bar in the central regions. This study became possible due to the recent completion of a large database on open clusters by our group. The birthplaces of the clusters are determined by two methods: one that assumes that the orbits are circular, and the other by integrating the orbits in the Galactic potential for a time equal to the age of the clusters. We selected in the database a sample of 212 clusters for which proper motions, radial velocities, distances, and ages are available, or of 612 clusters that have ages and distances available. We tested different assumptions concerning the rotation curve and the radius R_0 of the solar orbit. Our results confirm that a dominant fraction of the open clusters are formed in spiral arms, and that the spiral arms rotate like a rigid body, as predicted by the classical theory of spiral waves. We find that the corotation radius, R_c, is close to the solar Galactic orbit ($R_c/R_0 = 1.06 \pm 0.08$). This proximity has many potentially interesting consequences, such as a better preservation of life on the Earth and a new understanding of the history of star formation in the solar neighborhood, and of the evolution of the abundance of elements in the Galactic disk.

Subject headings: Galaxy: disk — Galaxy: kinematics and dynamics

1. INTRODUCTION

According to the classical theory of galactic spiral waves proposed by Lin & Shu (1964) and Lin et al. (1969), spiral arms are restricted to the interval between the inner and outer Lindblad resonances (ILR and OLR), where the pattern angular velocity Ω_p equals $\Omega \mp \kappa/2$, where Ω is the angular rotation velocity of the disk and κ is the epicycle frequency. The spiral pattern is considered to rotate like a rigid disk, while the gas and stars present differential rotation. The radius where $\Omega = \Omega_p$, called the corotation radius, is situated between the ILR and the OLR. Since κ is a function of Ω and of its derivative $d\Omega/dr$ only (e.g., Binney & Tremaine 1987), given the rotation curve of the Galaxy, the position of the Lindblad resonances depends only on the pattern rotation speed.

The radii of those resonances and of corotation in our Galaxy have been a subject of controversy. Lin and his collaborators situated the corotation at the edge of the Galactic disk, at about 16 kpc from the center. Other authors, such as Amaral & Lépine (1997) and Mishurov & Zenina (1999), claimed that the corotation is close to the radius of the solar orbit, R_0. This view is supported by recent studies of metallicity gradients in the Galactic disk (Andrievsky et al. 2004; Mishurov et al. 2002). Yet another group of researchers believes that the spiral pattern rotates so fast that the corotation resonance is situated in the inner part of the Galaxy at $r \approx 3$–4 kpc and the OLR is located close to the Sun (e.g., Weinberg 1994; Englmaier & Gerhard 1999; Dehnen 2000). In parallel with the quasi-stationary models just mentioned, which are variations of the model of Lin & Shu, there are quite different interpretations of the spiral structure, such as those of Binney & Lacey (1988) and of Sellwood & Binney (2002), who consider that the arms are constituted by a series of transient waves with different pattern velocities (and consequently different corotation radii), and that of Seiden & Gerola (1979), who argue that the arms are not density waves but the result of a stochastic self-propagating star formation process.

It is therefore an important step in the understanding of the spiral structure to firmly establish the rotation velocity of the spiral pattern in the Galaxy, as well as to verify whether different arms have the same velocity. In this paper we present a new method to measure the velocity of the spiral arms, based on the orbits of a sample of open clusters, which have known distances, space velocities, and ages.

2. THE OPEN CLUSTERS CATALOG

We make use of the *New Catalogue of Optically Visible Open Clusters and Candidates* published by Dias et al. (2002a) and updated by Dias et al. (2003).[3] This catalog updates the previous catalogs of Lyngä (1987) and Mermilliod (1995). The present version of the catalog contains 1689 objects, of which 599 (35.5%) have published distances and ages, 612 (36.2%) have published proper motions (most of them determined by our group; Dias et al. 2001, 2002b), and 234 (13.8%) have radial velocities.

3. BASIC ASSUMPTIONS

The basic assumption is that star formation, and in particular open cluster formation, takes place only (or almost only) in spiral arms. This follows from the ideas of Roberts (1969), Shu et al. (1972), and many others, according to whom the shock waves occurring in spiral arms are the triggering mechanism of star formation. There is observational evidence that this is true in external spiral galaxies, where we see the H II regions and massive stars concentrated in spiral arms. The fact that young

[1] Instituto de Física de São Carlos, Universidade de São Paulo, Caixa Postal 369, 13560-970 São Carlos, SP, Brazil.

[2] Instituto de Astronomia, Geofísica e Ciências Atmosféricas, Universidade de São Paulo, Rua do Matão 1226, Cidade Universitária, 05508-900 São Paulo, SP, Brazil; jacques@iagusp.usp.br.

[3] Available at http://www.astro.iag.usp.br/~wilton.

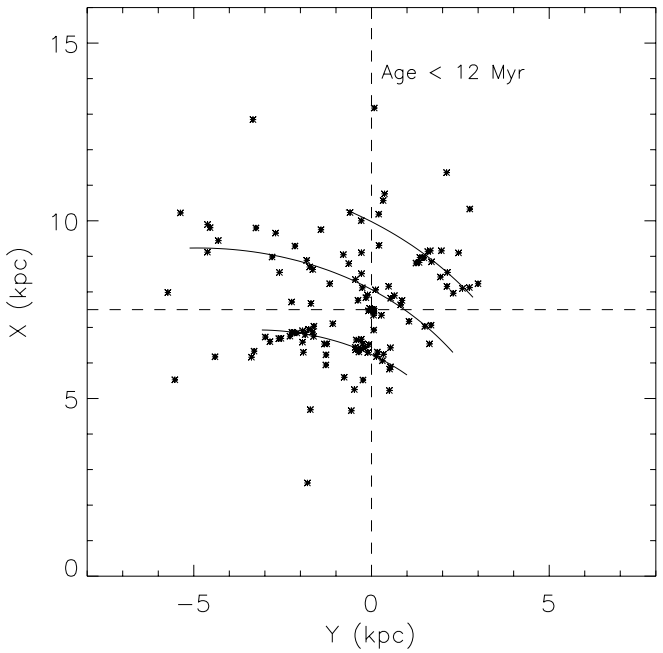

FIG. 1.—Sample of open clusters with age <12 Myr in the solar neighborhood. The Sun is at coordinates (0, 7.5); the Galactic center is at (0,0). Distances are in kpc. The usual *Y*- and *X*-axis centered on the Sun are shown as dashed lines.

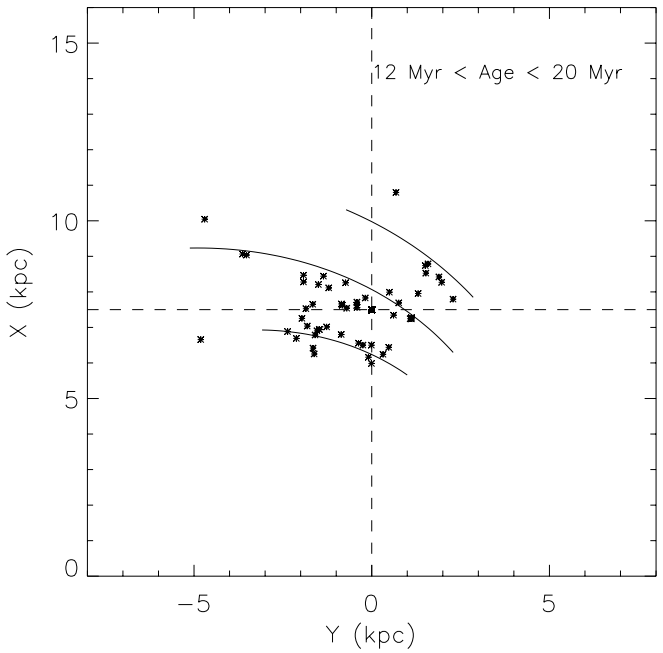

FIG. 3.—Present-day position of open clusters with 12 Myr < age < 25 Myr in the solar neighborhood. The lines represent approximately the present-day position of the arms, based on a younger sample.

open clusters are tracers of the spiral structure has been known for several decades (e.g., Becker & Fenkart 1970). The distribution of open clusters in the Galactic disk is shown in Figure 1, for clusters younger than 12 Myr, and in Figure 2, for clusters older than 30 Myr. It is clear that in about 20 Myr the open clusters drift away from the arms and fill the interarm regions. This work shows that the structure that has disappeared in Figure 2 can be retrieved by a proper correction of the cluster positions.

After their birth, the clusters follow Galactic orbits that can be easily calculated, since we know the Galactic potential.

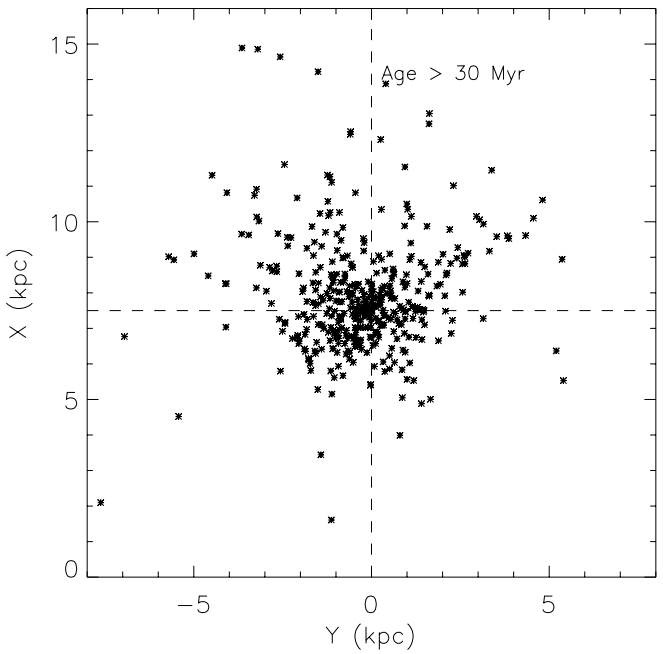

FIG. 2.—Sample of open clusters with age >30 Myr in the solar neighborhood.

Knowing the present-day space velocity components, we can integrate each orbit backward for a time interval equal to the age of the cluster and find where the clusters were born. The birthplace of each cluster indicates the position of a spiral arm at a past time equal to its age. In principle, it is not difficult to trace the motion of the arms. Our task is to find the most reliable way to extract this piece of information from the cluster data.

Before looking for precise methods to determine the corotation radius, we call attention to the fact that a direct inspection of the distribution of the clusters in the Galactic plane gives an approximate value of that radius, in a way that does not depend on any particular choice of a rotation curve or of a set of Galactic parameters. Let us compare Figure 1 with Figure 3: the difference between the two figures is the range of age of the clusters. The lines representing the position of the arms in Figure 1 (age < 12 Myr) are reproduced as guidelines in Figure 3 (12 Myr < age < 25 Myr). These lines represent approximately the present-day position of the arms. In Figure 3, most of the clusters associated with the Perseus arm (*outer arm*) are situated to the left of the line. In contrast, most of the clusters associated with the Sagittarius-Carina arm (*inner arm*) are situated to the right of the corresponding line. This means that the clusters that were born some 10–20 Myr ago, and since then are rotating around the Galactic center with about the velocity of the rotation curve, have rotated slower than the spiral pattern at the outer radii, and faster than the spiral pattern at the inner radii. This is what we expect to observe, if the corotation radius is between the two arms, that is, close to the Sun.

3.1. *Methods to Determine the Pattern Speed*

We propose two methods to trace back the orbits of the clusters and find their birthplace, which we call "true integration" and "circular rotation," and two methods to derive the rotation velocity of the arms, based on the birthplaces of the clusters; we call them "direct observation of pattern rotation" and "reconstruction of the present-day arms." In this work we present the two best combinations of these methods. We next

explain the reasons for the use of different methods to retrieve the birthplaces.

In principle, by performing a true integration of the orbit, using the observed space velocities as initial conditions, one takes into account the fact that the orbits are not precisely circular and obtains the best birthplace determinations. However, true integration is limited to the sample of clusters that have, in the catalog, distance, age, proper motion, and radial velocity. At the moment, this amounts to a total of 212 objects only. When we further restrict the sample to some narrow ranges of ages, as required by one of the methods discussed below, the available number of clusters becomes too small. Furthermore, one must remember that the components of the space velocities given in the catalog, in particular the radial velocities, are affected by errors, so that the initial conditions of the orbit integrations have uncertainties. These reasons led us to use simple circular rotation as an alternative method. In this case, the orbits of the clusters are supposed to be circular. The birthplaces are found by assuming that the clusters moved a distance equal to their age multiplied by their velocity, given by the rotation curve. Therefore, the only parameters needed to recover the birthplaces are distances and ages; in this case, the available sample in our database amounts to 599 objects.

3.1.1. *Direct Observation of Pattern Rotation (Method 1)*

The simplest way to proceed, once the birthplaces of the clusters have been obtained, is to directly observe the rotation of the pattern that they form, as illustrated in Figure 4. We first fitted segments of spiral arms (*dashed lines*) to the birthplaces of a sample of very young clusters (5–8 Myr, not shown). The adopted equation of spiral arms is $r = r_i \exp(k\theta + \phi_0)$, where r_i is the initial radius, θ is the galactocentric polar angle, with the direction of the Sun taken as the origin and increasing counterclockwise, ϕ_0 is the initial phase angle, and $k = \tan(i)$ is a constant related to the inclination i of the arm. We adjusted the parameters of the arms so as to obtain the best fit of the sample of youngest clusters; the arms are consistent with the well-known Sagittarius-Carina arm, the Local arm, and the Perseus arm. We noted that the exact expression used to describe the arms is not important; very similar results were obtained by fitting the arms with a second-order polynomial. The next step is to rotate the spiral segments around the Galactic center by varying ϕ_0, so as to obtain the best fit of an older sample (9–15 Myr; cluster birthplaces shown as stars or crosses, fitted solid lines); the rotation angle in this example is $\alpha = 8^\circ$.

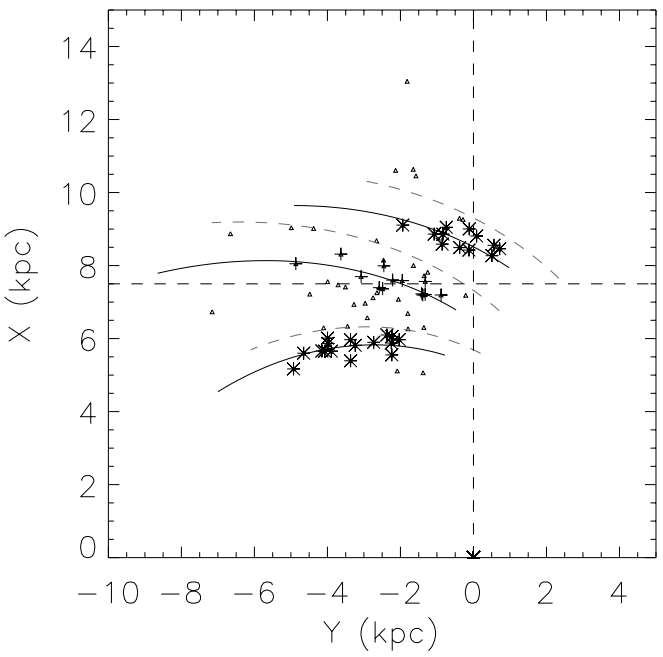

FIG. 4.—Birthplaces of the clusters with ages in the range 9–15 Myr (average 11.6 Myr) in the Galactic plane, obtained by direct rotation with a flat rotation curve with a velocity of 210 km s^{-1}. The dashed lines were fitted to a younger sample, not shown, with ages in the range 5–8 Myr (average 6.2 Myr); the solid lines are the same arms of the dashed line, rotated by 8° around the Galactic center. This angle is the best fit to the sample displayed. Different symbols have been used to indicate clusters belonging to each arm, or those more than 0.5 kpc from any arm (*small triangles*).

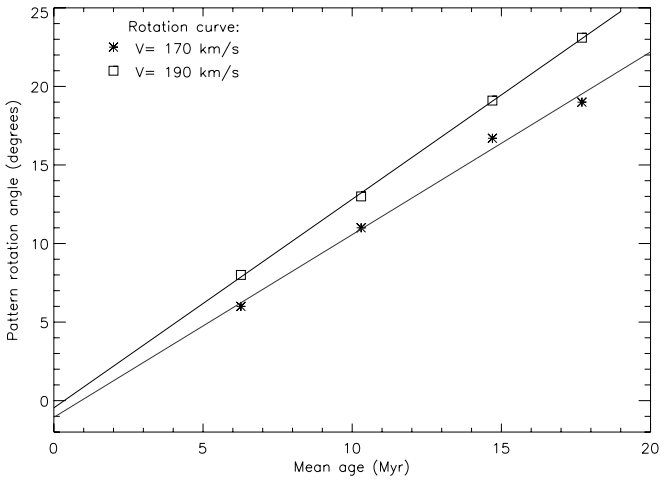

FIG. 5.—Rotation angle required to fit the birthplaces of samples of clusters of different ages with a spiral pattern that represents the present-day structure (method 1). In this example, the birthplaces were determined by direct rotation with two flat (constant velocity) rotation curves, with $V_0 = 170$ and $V_0 = 190$ km s^{-1}. The age range of the samples, in Myr, were 0–8 (average 6.27), 7–14 (average 10.3), 12–18 (average 14.7), and 15–22 (average 17.7).

We emphasize that Figure 4 is different from Figure 3 and previous ones, in the sense that we are plotting the birthplaces, not the present-day positions of the clusters. It is important to remark that a same rotation angle fits correctly the different arms, based on our sample of clusters, and within the precision of our measurements.

The variation of the rotation angle with the age of the samples is shown in Figure 5. The successive age ranges that were used are indicated in the caption. For each age range, the only parameter used to fit the pattern is the angle α, as in Figure 4. In order to maximize the number of clusters in each sample, we allowed a small overlap of the age ranges and adopted the birthplaces obtained by circular rotation of the clusters, as already explained.

The procedure to find the best-fit parameter α for each age range was as follows. For each of the three arms, we selected as belonging to the arm the clusters that are at a distance less than 0.5 kpc from it. For these clusters, we computed the sum of the components of the distances to the arm, in the Y-direction (defined here as the horizontal direction in the figure, which is about the direction of rotation of the Galaxy, for objects close to the Sun). When this sum is zero, this means that there are about the same number of clusters to the right and to the left of the arm, which gives the best fit.

The birthplaces depend obviously on the adopted rotation curve. As discussed later, we tested different rotation curves and values of R_0. In Figure 5 we compare the results for two flat rotation curves, with $V_0 = 170$ and $V_0 = 190$ km s^{-1}, for

$R_0 = 7.5$ kpc. The slopes of the fitted lines are $1\overset{\circ}{.}16$ and $1\overset{\circ}{.}33$ Myr^{-1}, respectively. It is an expected result that when we adopt a larger rotation velocity, the birthplaces are found more distant from the solar neighborhood, and a larger rotation velocity of the pattern is derived. Note that 1° Myr^{-1} is equivalent to 17 km s^{-1} kpc^{-1}; the derived corotation radii ($=V_0/\Omega_p$) are 8.6 and 8.4 kpc, respectively, in this example.

3.1.2. *Reconstruction of Spiral Arms (Method 2)*

Although it is usually accepted that young Galactic objects have near-circular orbits, it is important to check whether the hypothesis of circular motion can be responsible for systematic errors in the determination of the pattern rotation speed. For instance, it is expected that the shock waves in the spiral perturbation potential produce a braking the molecular clouds (and consequently of the recently formed stars) at Galactic radii smaller than the corotation radius, and an acceleration of the molecular clouds at larger radii. It is therefore necessary to perform experiments with exact integration of the orbits in order to take into account the initial velocity perturbation.

The method previously described to derive the pattern rotation velocity requires a sufficiently large number of clusters in each age bin. The second method that we propose here does not separate the clusters into age bins and makes use of a sample with a wide range of ages. It is convenient to work with the small sample of clusters for which it is possible to perform exact integration of the orbits.

In this method, as a first step, we find the birthplace of each cluster, integrating backward their orbits for time intervals T equal to their age, starting from the present-day initial conditions (positions and space velocities). The method of integration is discussed later. The birthplace of a cluster is supposed to represent a point of a spiral arm, a time T ago. If we rotate forward this point an angle $\Omega_p T$ around the Galactic center, we obtain a point situated on the present-day position of the arm. In this way, points corresponding to very different ages can be used to trace the present-day arms. The unknown is Ω_p. The best estimate of Ω_p is the one that gathers the maximum number of points close to the present-day position of the arms. In practice, the best value of Ω_p is found in an interactive mode, using a technique similar to that of the previous method. We select the points that are within 0.5 kpc of any of the three arms (to avoid mixing of arms), and we minimize the rms distance to the arms, varying Ω_p. However, we do not know a priori the present-day position of the arms, because there are almost no cluster younger than 5 Myr. Even if we selected a young sample, we would need to correct the observed positions, using Ω_p. Therefore, we use an interactive method: for each adopted Ω_p, we allow minor variations in the parameters describing the arms, in order to minimize the rms distance of the points to them. Next we compare the rms distances obtained with different values of Ω_p. We illustrate in Figure 6 the results obtained with this method, using a CO-based rotation curve (see below). The adjusted points were from the sample of clusters in the range 0–50 Myr. The same result is obtained if we use another range, such as 10–30 Myr. However, the absolute errors on the age tend to increase with the age, and it is preferable not to exceed 50 Myr. The derived value of Ω_p in the example is 25 ± 1 km s^{-1} kpc^{-1}, which correspond to a corotation radius of 8.2 ± 0.4 kpc, for $R_0 = 7.0$ kpc and $V_0 = 200$ km s^{-1}.

3.1.3. *Rotation Curves and Details of Orbit Integration*

Most of the open clusters in the catalog of Dias et al. (2002a, 2003) are situated at Galactic radii in the range $R_0 \pm 2$ kpc, so that our calculations only make use the portion of the rotation curve situated in this range. Since the rotation curve of the Galaxy is known to be relatively flat close to the Sun, a linear approximation of it is sufficient, in this interval. The only important parameters are the rotation velocity of the local standard of rest (LSR), V_0, and the slope of the rotation curve, $(dV/dR)_{R_0}$. These parameters are linked together and with the value of R_0 through the Oort constants A and B, which are determined by observations [$V_0/R_0 = A - B$, $(dV/dR)_{R_0} = -A - B$]. The R_0 value 8.5 kpc, recommended by the International Astronomical Union, is often used in the literature with $V_0 = 220$ km s^{-1}, which corresponds to $A - B = 26$ km s^{-1} kpc^{-1} (e.g., Binney & Tremaine 1987). This value of $A - B$ seems to be well established and is confirmed by recent observations of a different nature (Kalirai et al. 2004) that give 25.3 ± 2.6 km s^{-1} kpc^{-1}. Recent works often adopt $R_0 = 7.5$ kpc (Racine & Harris 1989; Reid 1993, and many others). The shorter scale is supported by very long baseline interferometry (VLBI) observations of H_2O masers associated with the Galactic center. Keeping the same value for $A - B$, the corresponding V_0 would be 195 km s^{-1}. We note that Olling & Dehnen (2003) argue that the rotation curve is flat ($A = -B$), but usually, the rotation curve is considered to be decreasing near the Sun, with $-A - B$ about -3 km s^{-1} kpc^{-1} (Binney & Tremaine 1987).

We calculated Ω_p for a grid of points in the R_0-V_0 plane with R_0 in the range 6.5–8.5 kpc, in steps of 0.5 kpc, and V_0 in the range 160–220 km s^{-1}, in steps of 10 km s^{-1}. For each point of the grid we used a rotation curve similar to that of Clemens (1985), adapted to the corresponding values of R_0 and V_0. The original curve obtained by Clemens assumed $R_0 = 8.5$ kpc and $V_0 = 220$ km s^{-1}. Each data point of the rotation curve corresponds to the velocity at the subcentral point; it is the maximum velocity in the observed spectrum, minus the projection of the velocity of the LSR on the line of sight [$V_0 \sin(l)$]; the Galactic radius is such that $l = \arcsin(R/R_0)$. With new values of R_0 and V_0, for the same longitude we have the same observed velocity (the observational data are unchanged), but it corresponds to a different Galactic radius, and to a different velocity at the subcentral point. For each point of the grid we recalculated the data of the rotation curve and fitted them with a simple analytical expression, to be used in the following calculations. An

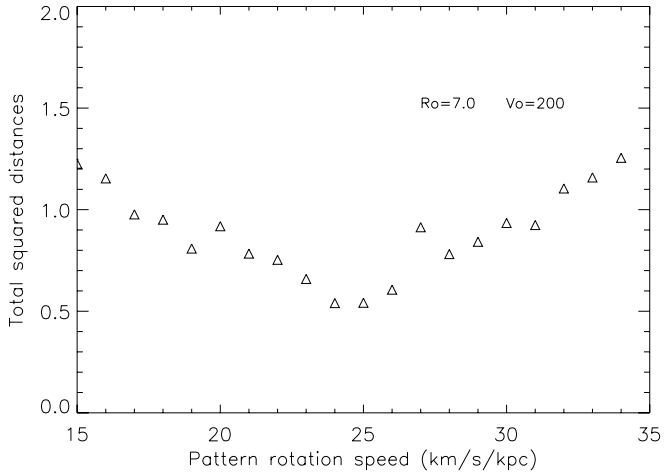

FIG. 6.—Procedure to find the best estimate of pattern rotation velocity Ω_p (method 2). The best value (25.0 km s^{-1} kpc^{-1}) is given by the minimum of the sum of the squared distances from the points to the fitted arms. This example corresponds to $R_0 = 7.0$ kpc and $V_0 = 200$ km s^{-1}; the birthplaces (first step of method 2) were determined by orbit integration using the corresponding CO-based rotation curve.

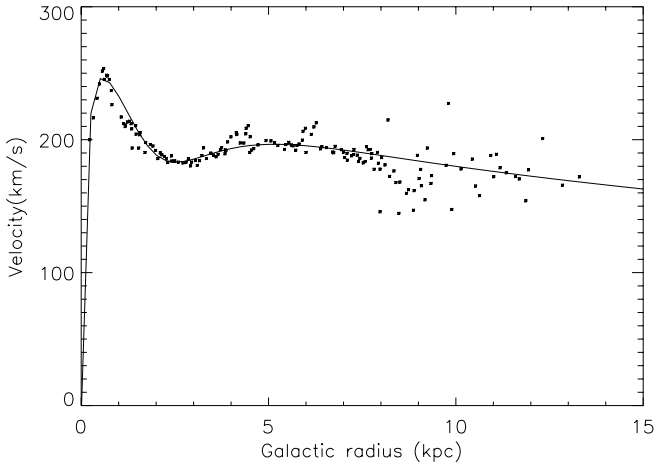

FIG. 7.—CO-based rotation curve of the Galaxy, with Clemens (1985) data corrected for $R_0 = 7.5$ kpc and $V_0 = 190$ km s^{-1}. The curve is fitted by the expression $V = 228\ \exp\left[-r/50 - (3.6/r)^2\right] + 350\ \exp(-r/3.25 - 0.1/r)$.

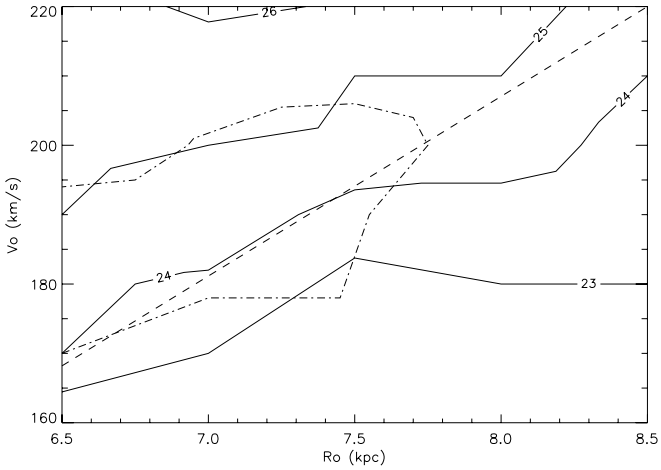

FIG. 8.—Contour map of the pattern rotation speed Ω_p obtained with CO-based rotation curves. The dashed line represents the locus of the best estimate of the ratio V_0/R_0, based on the Oort constants. The dash-dotted contour represents the region where the best fits were obtained.

example of these CO-based curves, for $R_0 = 7.5$ kpc and $V_0 = 190$ km s^{-1}, is shown in Figure 7. The fitted curve has a linear behavior close to the Sun, with a slope of about -3.3 km s^{-1} kpc^{-1}. For this curve in particular, both V_0/R_0 and $(dV/dR)_{R_0}$ are in agreement with the best estimates of Oort constants.

A property of the above method to derive rotation curves is that the slope of the curves depends strongly on the adopted value of V_0; for instance, for $R_0 = 7.5$ kpc, and for $V_0 = 160$ km s^{-1}, the curve is strongly decreasing outward, while for $V_0 = 220$ km s^{-1} it increases outward. In order to test curves that are not so much restricted by the CO-based data, we also performed the calculations for flat curves with different values of V_0.

To perform numerical integration of the orbits, the observed radial velocities and proper motions were corrected for differential rotation before being converted to radial and tangential velocity components in the local Galactic system. The corrections were made by computing, for the longitude and distance of each cluster, the expected radial velocity and proper motion in the frame of the LSR, assuming that the cluster presents pure circular rotation obeying the rotation curve considered. The differences between the observed velocities and the expected ones give the excess velocities that are the initial perturbation velocities in the orbit integration program. This direct correction for differential rotation is not very different from the approximation based on Oort constants (e.g., Carraro & Chiosi 1994), but it is correct even for clusters situated at large distances. Another correction is the transformation of the velocities to the LSR; we first assumed that the Sun has a velocity of 22 km s^{-1} in the direction $l = 61\overset{\circ}{.}4$, $b = 20\overset{\circ}{.}4$ (Abad et al. 2003).

However, we found in performing the calculations for our method 2 that the minima of the sum of the squared distances of the points to the arms (Fig. 6) were deeper and better defined if we applied to the observed velocities a velocity correction of 10 km s^{-1} in the direction of Galactic rotation. In other words, we consider that the LSR has a velocity $(V_0) - 10$ km s^{-1} in the frame of the Galaxy. This probably means that our initial choice of solar velocity component $V_\odot$ in the direction of Galactic rotation, in the transformation to the LSR, was not the most appropriate one. While there is good agreement between different authors on the values of the other two components, $U_\odot$ and $W_\odot$, $V_\odot$ is known to depend of the color of the stars taken as a reference for the LSR (Dehnen & Binney 1998). While $V_\odot$, recommended by Abad et al. (2003), is 18 km s^{-1}, one can see in the work of Dehnen & Binney that a value of 8 km s^{-1}, obtained from young stars, is closer to the equilibrium with the potential of the Galaxy. We present in Figures 8 and 9 the contour maps of Ω_p and of R_c/R_0 that we obtained for the grid of points.

One has to be cautious in interpreting the contours, since the errors on individual measurements of Ω_p are of about 1 km s^{-1} kpc^{-1}, which is about the separation between the contour lines. Nevertheless, we can observe the general trends: Ω_p increases with V_0, for a fixed R_0, and decreases slowly with R_0, for a fixed V_0. The R_c/R_0 contour lines are almost parallel to the constant V_0/R_0 line. We found minima in the rms distances of the points to the arms for all the points of the grid; however, the minima were deeper in the region indicated by the dot-dashed contour in the two figures. The contour corresponds to a rms distance of 0.1 kpc, at the minimum. Typically in this region 80% of the points (rotated birthplaces) are found within 0.4 kpc of one of the three arms, while the spacing between arms is about 2 kpc.

3.1.4. *Errors Associated with Cluster Ages*

In a large sample such as our database, different methods have been used by different authors to determine ages. In most cases, the age are obtained by isochrone fitting, which depends critically on the adopted reddening, and sometimes relies on a

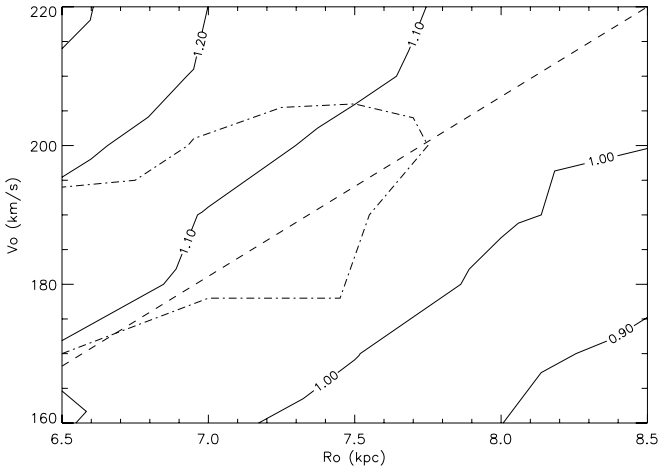

FIG. 9.—Contour map of the ratio of corotation radius to solar orbit radius, R_c/R_0, based on the same analysis of Fig. 8.

small number of stars. In other cases, the spectral type of turn-off stars is determined through spectroscopy. We follow here the discussion by de la Fuente Marcos & de la Fuente Marcos (2004), who compared age determinations from different sources for a sample of well-studied clusters and found an average error of 22%. Although that study focuses on an older age range, we investigated the effect of a random age error of the order of 20%. In a number of experiments, after finding the value of Ω_p by the method illustrated in Figure 6, we multiplied the ages of the clusters by a factor randomly distributed between 0.8 and 1.2, and then redetermined Ω_p. The minimum becomes less sharply defined, but no systematic deviation is introduced. In general, our method is not excessively dependent on the ages, since the age of a cluster is used in one direction to find the birthplace of a cluster, and in the opposite direction to rotate the corresponding point to its position on the present-day arm. We adopt as the error on the measurement of Ω_p the error on the determination of the minimum as in Figure 6, which already includes the effect of random errors on the ages.

4. RESULTS AND CONCLUSIONS

The Galactic corotation radii R_c derived in this work are summarized in Figure 9 and in Table 1. In Figure 9 we present the results for a grid of points that covers the reasonable range of values of R_0 and V_0 for the Galaxy. It can be seen that along the line $V_0/R_0 = 25.9$ km s^{-1} kpc^{-1}, which is the locus of the most probable sets of R_0 and V_0, according to the accepted values of Oort constants A and B, R_c/R_0 varies between about 1.05 and 1.08. Interestingly, the region of the grid where our method 2 gives the best results (better reconstruction of the spiral arms) almost coincides with the region of best fitting for R_0 and V_0, in the work of Olling & Merrefield (1998). Our results reinforce the conclusions of that paper in favor of a short distance scale for the Galaxy. In Table 1 we present results obtained with our method 1 (direct measurement of the rotation angle required to fit clusters of different age ranges), or with method 2 (reconstruction of the arms), but using flat rotation curves instead of CO-based curves.

Typical errors on individual determinations are about ± 0.3 kpc. The values of R_c that we obtain with different methods and different subsamples of open clusters are quite consistent: R_c is slightly larger than R_0 in almost all determinations, and R_c/R_0 is situated in the interval 0.95–1.14, the best estimate being $R_c/R_0 = 1.06 \pm 0.08$; R_c is roughly proportional to the adopted value of R_0 and depends very little on V_0, and R_c depends slightly on the slope of the adopted rotation curve. For instance, imposing a flat rotation curve to a case with $V_0 = 170$ km s^{-1} (first example in Table 1) produces R_c/R_0 larger than the average value. Within the precision of our method and the limitations of our sample, the three main arms seen in the solar neighborhood present the same rotation velocity. Our results strongly favor the idea that the spiral pattern rotates like a rigid body. The pattern rotation speed is 24 km s^{-1} kpc^{-1}, which situates the ILR and OLR at 2.5 and 11.5 kpc, respectively, for $R_0 = 7.5$ kpc and $V_0 = 190$ km s^{-1}. Considering that the Galaxy has an important 4-arm mode, the corresponding ILR and OLR ($\Omega \pm \kappa/4$) are at about 5 and 10 kpc. For a large majority of the open clusters, we can retrieve a birthplace that coincides with the position of a spiral arm at the epoch of its birth. Possibly others can be explained by errors in the age determination or by the existence of subarm structures between the main arms. This observation, which is not feasible in external galaxies, gives robust support to the view that spiral arms are the triggering mechanism of star formation.

TABLE 1
COROTATION RADIUS OBTAINED WITH DIFFERENT ROTATION CURVES

Curve	Method	R_0 (kpc)	V_0 (km s^{-1})	R_c (kpc)
Flat	Circular rotation	7.5	170	8.6
Flat	Circular rotation	7.5	190	8.4
Flat	Circular rotation	7.5	210	8.0
Flat	Circular rotation	8.5	190	8.8
Flat	Circular rotation	8.5	210	9.5
CO-based.....	Circular rotation	7.5	170	7.5
CO-based.....	Circular rotation	7.5	190	7.9
Flat	True integration	8.5	170	8.1
Flat	True integration	8.5	190	8.6

NOTE.—The results obtained with 35 different CO-based curves and true integration presented in Figs. 8 and 9 are not included in the table.

The proximity of the Sun to the corotation radius means that it has a small velocity with respect to the spiral arms, and that long periods of time elapse between successive crossings of the spiral arms. The crossing of spiral arms is a probable explanation for the existence of peaks in the history of star formation in the solar neighborhood (Rocha-Pinto et al. 2000; de la Fuente Marcos & de la Fuente Marcos 2004). Furthermore, the encounters with spiral arms, with the larger probability of nearby supernovae explosions and of gravitational perturbation of the Oort cloud, making more objects like comets to fall toward the inner solar system, could be associated with events of mass extinction of terrestrial (or extraterrestrial) life (Leitch & Vasisht 1998). Finally, the corotation radius is often considered to be associated with a minimum of star formation. If the star formation rate (SFR) is related to the rate at which the interstellar gas is introduced into the arms, which can be viewed as gas-to-star transformation machines, a recipe that has been proposed is SFR $\propto |\Omega - \Omega_p|$ (Mishurov et al. 2002). The minimum in the star formation rate close to the Sun is a condition that favors the survival of life on the Earth. Marochnik (1983) already presented many years ago the hypothesis that the corotation circle is a region where we should find systems similar to the solar system. Moreover, a radius with a minimum of star formation rate must correspond to a minimum of metallicity, since the enrichment of the interstellar medium in metals is related to the death of short-lived massive stars. These concepts are essential to understand the bimodal gradient of abundance of different elements in the disk (Andrievsky et al. 2004).

The work was supported in part by the Sao Paulo State agency FAPESP (fellowship 03/12813-4).

REFERENCES

Abad, C., Vieira, K., Bongiovanni, A., Romero, L., & Vicente, B. 2003, A&A, 397, 345
Amaral, L. H., & Lépine, J. R. D. 1997, MNRAS, 286, 885
Andrievsky, S. M., Luck, R. E., Martin, P., & Lépine, J. R. D. 2004, A&A, 413, 159
Becker, W., & Fenkart, R. B. 1970, in IAU Symp. 38, The Spiral Structure of Our Galaxy, ed. W. Becker & G. I. Kontopoulos (Dordrecht: Reidel), 205
Binney, J. J., & Lacey, C. 1988, MNRAS, 230, 597
Binney, J. J., & Tremaine, S. 1987, Galactic Dynamics (Princeton: Princeton Univ. Press)
Carraro, G., & Chiosi, C. 1994, A&A, 288, 751
Clemens, D. P. 1985, ApJ, 295, 422
Dehnen, W. 2000, AJ, 119, 800

Dehnen, W., & Binney, J. J. 1998, MNRAS, 298, 387
de la Fuente Marcos, R., & de la Fuente Marcos, C. 2004, NewA, 9, 475
Dias, W. S., Alessi, B. S., Moitinho, A., & Lépine, J. R. D. 2002a, A&A, 389, 871
———. 2003, in Proc. Galactic and Stellar Dynamics, ed. C. M. Boily et al. (Les Ulis: EDP Sciences), 195
Dias, W. S., Lépine, J. R. D., & Alessi, B. S. 2001, A&A, 376, 441
———. 2002b, A&A, 388, 168
Englmaier, P., & Gerhard, O. 1999, MNRAS, 304, 512
Kalirai, J. S., et al. 2004, ApJ, 601, 277
Leitch, E. M., & Vasisht, G. 1998, NewA, 3, 51
Lin, C. C., & Shu, F. H. 1964, ApJ, 140, 646
Lin, C. C., Yuan, C., & Shu, F. H. 1969, ApJ, 155, 721
Lyngä, G. 1987, A Computer Readable Catalogue of Open Cluster Data (5th ed.; Strasbourg: CDS)
Marochnik, L. S. 1983, Ap&SS, 89, 61
Mermilliod, J. C. 1995, in Information and On-Line Data in Astronomy, ed. D. Egret & M. A. Albrecht (Dordrecht: Kluwer), 127
Mishurov, Yu. N., Lépine, J. R. D., & Acharova, I. A. 2002, ApJ, 571, L113
Mishurov, Yu. N., & Zenina, I. A. 1999, A&A, 341, 81
Olling, R. P., & Dehnen, W. 2003, ApJ, 599, 275
Olling, R. P., & Merrefield, M. R. 1998, MNRAS, 297, 943
Racine, R., & Harris, W. E. 1989, AJ, 98, 1609
Reid, M. J. 1993, ARA&A, 31, 345
Roberts, W. W. 1969, ApJ, 158, 123
Rocha-Pinto, H. J., Scalo, J., Maciel, W. J., & Flynn, C. 2000, ApJ, 531, L115
Seiden, P. E., & Gerola, H. 1979, ApJ, 233, 56
Sellwood, J. A., & Binney, J. J. 2002, MNRAS, 336, 785
Shu, F. H., Millione, V., Gebel, W., Yuan, C., Goldsmith, D. W., & Roberts, W. W. 1972, ApJ, 173, 557
Weinberg, M. D. 1994, ApJ, 420, 597